Pediatr Radiol (2009) 39:1080–1086
DOI 10.1007/s00247-009-1354-y

ORIGINAL ARTICLE

Imaging of congenital mesoblastic nephroma with pathological correlation

Gulraiz Chaudry · Antonio R. Perez-Atayde · Bo Yee Ngan · Munire Gundogan · Alan Daneman

Received: 7 April 2009 / Revised: 20 June 2009 / Accepted: 26 June 2009 / Published online: 21 July 2009

Abstract
Background There are a variety of imaging findings for congenital mesoblastic nephroma (CMN) and two main pathological variants: classic and cellular.
Objective To determine whether imaging findings in children can predict the likely pathological variant.
Materials and methods We reviewed imaging in children with pathology-proven CMN. Imaging findings correlated with gross and histological appearance.
Results In 15 boys and 15 girls with CMN, US was performed in 27, CT in 19, and MRI in 7. Cystic components were readily identified on US; central hemorrhage was better differentiated on CT. MRI demonstrated high sensitivity for both. Histology confirmed classic CMN in 13 children, cellular CMN in 14 and "mixed" CMN in 3. Age at presentation was significantly higher in children with the cellular variant. Of 15 solid or predominantly solid tumors and 10 lesions with a hypoechoic ring, 12 and 7, respectively, had pathology consistent with classic CMN. In contrast, five of seven with intratumoral hemorrhage and all with a large cystic/necrotic component had pathology consistent with the cellular variant.
Conclusion The imaging appearance of CMN is often determined by the pathological type of tumor. Findings suggestive of the classic variant include a peripheral hypoechoic ring or large solid component. In comparison, cystic/necrotic change and hemorrhage is much more common in cellular CMN.

Keywords Mesoblastic nephroma · CMN · Imaging · Pathological correlation · Children

G. Chaudry (✉)
Department of Radiology, Children's Hospital Boston,
300 Longwood Ave,
Boston, MA 02115, USA
e-mail: gulraiz.chaudry@childrens.harvard.edu

A. R. Perez-Atayde
Department of Pathology, Children's Hospital Boston,
Boston, MA, USA

B. Y. Ngan
Department of Pathology, The Hospital for Sick Children,
Toronto, ON, Canada

M. Gundogan · A. Daneman
Department of Diagnostic Imaging,
The Hospital for Sick Children,
Toronto, ON, Canada

Introduction

Congenital mesoblastic nephroma (CMN) is the most commonly occurring renal tumor in the first year of life. It was originally described by Bolande et al. [1] as a leiomyoma-like tumor with excellent prognosis with nephrectomy alone. However, later studies established that a spectrum of disease exists, with two main pathological variants: the classic CMN and the more aggressive cellular CMN [2, 3]. The cellular variant is distinguished by hemorrhage and necrosis in the tumor, with invasion of perirenal fat and adjacent organs as well as evidence of local recurrence [2]. Histologically, the more aggressive tumor is characterized by increased cellularity, plump cells with nuclear pleomorphism, high nuclear/cytoplasmic ratio and frequent mitotic figures [2]. Although previous studies have highlighted some important differences in the US appearances between the two main variants [3, 4], there have been only isolated reports on the CT and MRI findings [5, 6].

We retrospectively reviewed the imaging and pathology in children presenting with CMN in two children's hospitals

over a 15-year period. US, CT and MR images were reviewed and correlated with the pathology findings.

Materials and methods

The study was approved by the Institutional Review Boards of both institutions. All infants with a radiological diagnosis of CMN in the last 15 years were initially identified. These cases were then correlated with pathology reports obtained after nephrectomy. All of the imaging performed in these infants was then reviewed. The clinical charts were also obtained to document presentation, treatment and follow-up. Finally, the imaging findings were correlated with gross pathology and histology. Statistical analysis was performed using Student's *t*-test.

Three of the CT scans and four of the US studies were performed at outside institutions. The remainder of the examinations were performed in the two institutions involved in the study. The US images were obtained using a number of different machines, but predominantly with Acuson Sequoia systems (Siemens Medical Solutions, Erlanger, Germany) and ATL 500 systems (Philips Medical Systems, Best, The Netherlands). As per routine in both institutions, a full abdominal US scan was performed in all patients. In all studies, 2-D and color Doppler images were obtained.

CT scans were performed using single-slice, 8-slice or 32-slice helical scanners (GE Medical Systems, Milwaukee, WI). Intravenous contrast agent was administered in all children. In five children, this was preceded by a non-contrast scan of the abdomen. A 1.5-T MRI scanner (GE Medical systems, Milwaukee, WI) was used to obtain the MR images in seven children. In all of these children, a multiplanar, multisequence study was performed, with and without gadolinium contrast enhancement. All CT and MRI studies were performed within 1 week of the US scan.

The pathology was obtained following nephrectomy in all 30 patients. Gross pathological analysis was followed by light microscopy and, in some cases, electron microscopy. Immunohistochemical staining and molecular genetic analysis were also carried out as indicated.

Results

A total of 30 children met the inclusion criteria for the study with a proven pathological diagnosis of CMN. There were 15 girls and 15 boys ranging in age from 1 day to 23 months. In 12 of the children the tumor had been detected on an antenatal sonogram. The remainder presented with a palpable abdominal mass. A single tumor was identified in all children. The tumor arose from the left kidney in 14 children and the right in 16. A nephrectomy was performed in all 30 patients, within a month of diagnosis in 28.

Pathological analysis of the nephrectomy specimens demonstrated findings consistent with classic CMN in 12 children. This included two specimens with predominantly (>75%) classic features, but focal areas of increased mitosis. The gross appearance in these 12 specimens was that of a predominantly solid, trabeculated yellow tumor with minimal hemorrhage or cystic/necrotic change (Fig. 1). Histologically, uniform, elongated, spindle-shaped cells arranged in bundles were seen, with trapped normal-appearing glomeruli and tubules (Fig. 1). The more aggressive cellular variant was diagnosed in 15 children. On examination of the gross specimens, 14 of 15 showed cystic/necrotic change with focal areas of hemorrhage (Fig. 2). Microscopic features seen in these specimens were nuclear atypia, high mitotic rate and increased cellularity (Fig. 2). Molecular analysis in six tumors demonstrated a t (12;15) translocation, consistent with cellular CMN. Three tumors were described as "mixed," with no predominant

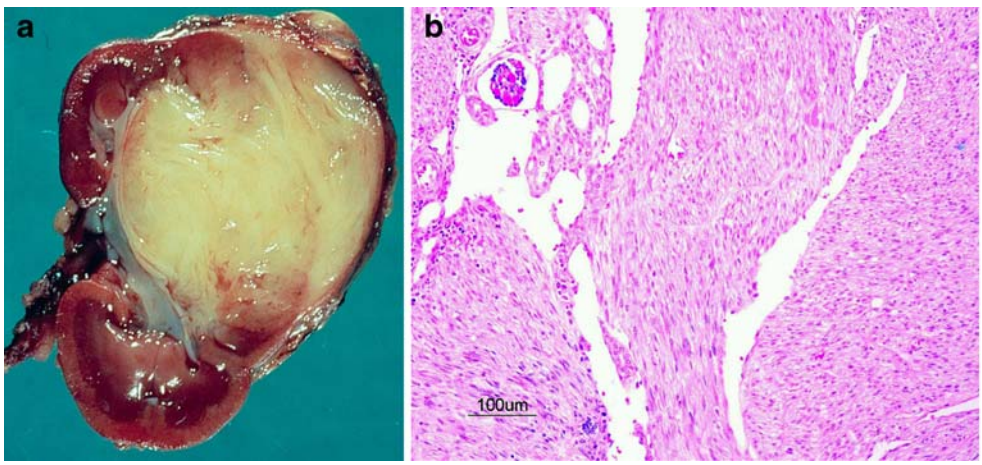

Fig. 1 Classic CMN. **a** A solid yellow tumor is seen arising from the upper pole of the kidney. **b** Histology (H&E stain). Uniform fascicles of spindled cells resembling fibroblasts or myofibroblasts are seen. The mitotic rate is low. Relatively abundant collagen is present in this patient's tumor

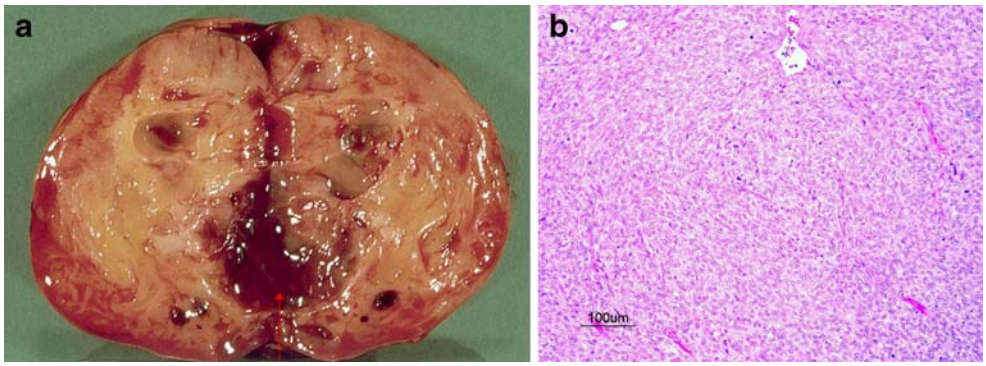

Fig. 2 Cellular CMN. **a** Multiple areas of cystic change are seen, together with central hemorrhage (*arrow*). **b** Histology (H&E stain). Fusiform to ovoid high densities of spindle cells impart a sarcomatous appearance. There is a higher mitotic rate

variant identified. The tumor extended outside the capsule in one of the "mixed" tumors. In addition, two other children with cellular CMN had evidence of local invasion, with extracapsular extension of the tumor.

The age at presentation of the children with the classic variant was (mean±SD) 6.6±9.4 days, and of those with the cellular variant was 121±236 days. The difference in age was statistically significant (P=0.04). Although cellular tumors were diagnosed as early as the first day of life, all children presenting with a tumor beyond 1 month of age had either the mixed or cellular variant. Following nephrectomy, local recurrence was seen in the retroperitoneum in two children. In both, pathology was consistent with cellular CMN and recurrence occurred within 6 months of resection.

An abdominal radiograph was obtained in 11 infants. An abdominal US scan was performed in 27 of the children, of whom 16 also subsequently underwent a CT examination of the abdomen. In addition, a CT scan was performed in three children as their primary imaging investigation, all at outside institutions. An MRI scan was performed in seven children, with precontrast T1 and fluid-sensitive T2/inversion recovery sequences and post-contrast T1 sequences performed in at least two planes.

The abdominal radiograph demonstrated nonspecific abdominal distension in all 11 children, with displacement of the bowel loops noted in two (Fig. 3). There was no evidence of calcification or bowel obstruction on any of the images.

In the 27 infants who underwent US, the mass identified was mixed solid and cystic in 8, predominantly (>75%) cystic in 4, predominantly (>75%) solid in 6, and completely solid in 9 (Fig. 4). The findings were consistent with gross pathological appearances. In particular, all areas of cystic/necrotic change seen on gross pathological specimens were readily identified on US. On histology, all four predominantly cystic masses were consistent with cellular CMN. Six of the eight tumors with mixed solid and cystic components were also diagnosed as cellular CMN or mixed. In comparison, seven of the nine completely solid masses and five of the six predominantly solid tumors had the histological appearance of classic CMN. A hypoechoic ring was identified at the periphery of ten of the tumors (Fig. 5), seven of which had pathology consistent with classic CMN.

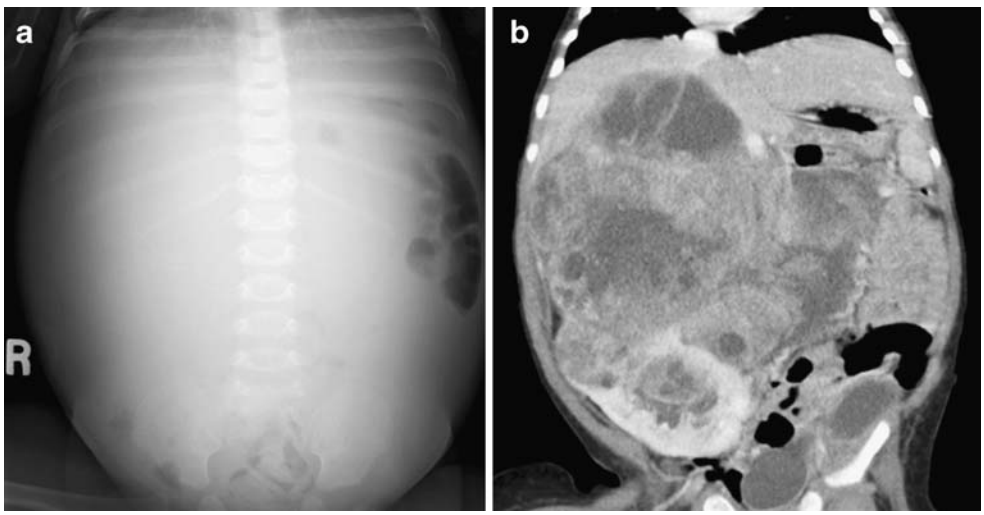

Fig. 3 Large abdominal mass in a 5-month-old boy. **a** Abdominal radiograph. There is marked abdominal distension with displacement of bowel to the left. **b** Contrast-enhanced CT of the abdomen, coronal reformatted image. A large, heterogeneous mass is seen arising from the upper pole of the right kidney, with areas of cystic/necrotic change and enhancement of the solid components. Pathology was consistent with a cellular CMN

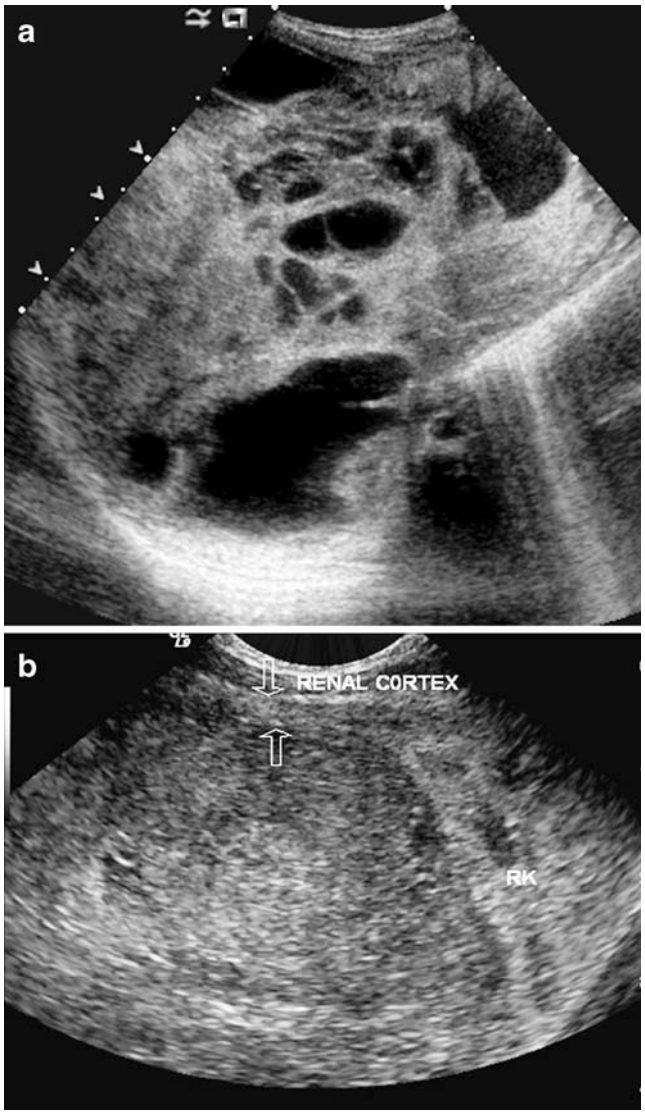

Fig. 4 US findings. **a** A heterogeneous tumor with focal cystic spaces is noted on the right. Histology was consistent with cellular CMN. **b** A solid mass is seen in the upper pole of the right kidney. Histology confirmed a classic CMN

Among the 16 children who had US and CT examinations, there was no discrepancy in the findings in 12 children. Heterogeneity in attenuation was seen in all but one child. Cystic/necrotic change was better appreciated on US and, in one child, a cystic area seen on US was not resolved on CT. In seven children, areas of heterogeneity on US were more readily appreciated as hemorrhagic foci on CT (Fig. 6). As a preliminary noncontrast study was only performed in a minority, this may be an underestimate. Five of the seven tumors with intratumoral hemorrhage demonstrated on CT were identified as the cellular variant. Heterogeneous enhancement of the mass was seen in the solid areas (Fig. 6). The three children with a CT scan as their initial postnatal imaging investigation all had focal

Fig. 5 A 12-day-old infant with antenatal diagnosis of a right renal mass. A peripheral hypoechoic ring is seen. Pathology was consistent with classic CMN

areas of low attenuation consistent with cystic/necrotic change. All three were later diagnosed as cellular CMN.

An MRI scan was performed in seven children. Six of these infants had a prenatal diagnosis of a renal mass and all of the studies were performed within the first week of life. A postnatal US scan was performed prior to the MRI scan in all infants. Multiplane, multisequence MRI examinations were performed. On the sequence before gadolinium administration the solid components of the tumor were of low signal on T1 and high signal on T2 in comparison to the normal renal parenchyma on the other side (Fig. 7). In three children a focal area of high intensity was seen on T1, consistent with hemorrhage, which was not appreciated on US in two (Fig. 7). The sequences after gadolinium administration demonstrated variable heterogeneous enhancement of the solid components of the mass (Fig. 7). As a result of the small number of patients, there were no statistically significant differences ($P>0.05$) in the enhancement patterns of the different histological types of tumors.

Discussion

CMN is rare, representing only 3–6% of renal tumors occurring in childhood [4]. However, it still remains the most common renal tumor in the first few months of life [7]. As early as 1970, Beckwith [8] had predicted that a pathological spectrum existed, with classic CMN at one end and malignant spindle cell sarcomas at the other. Joshi et al. [2] then provided criteria for selecting a more aggressive subgroup that they termed “cellular CMN.” Gross features of these tumors included a soft mass with

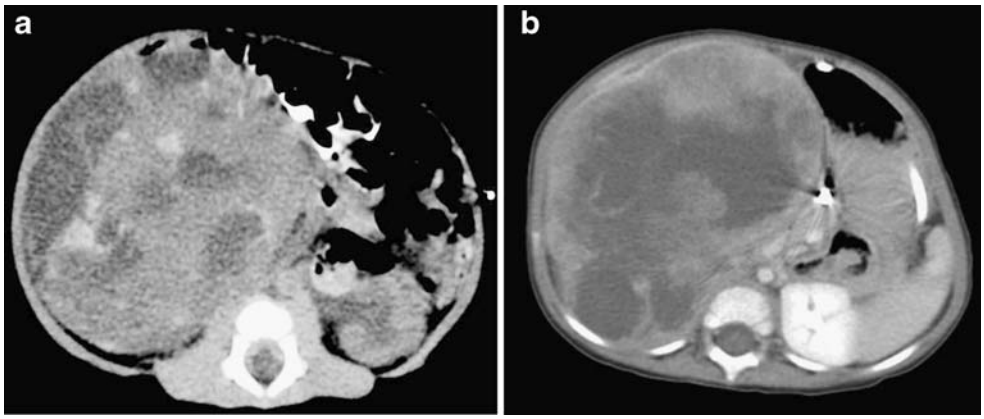

Fig. 6 CT scan in two infants with large, right-sided renal tumors. **a** Noncontrast CT image reveals multiple areas of high attenuation in the right-sided mass, consistent with hemorrhage. **b** Contrast-enhanced CT image in a different child demonstrates a complex mass in the right kidney with heterogeneous enhancement of the solid components. Both children were subsequently diagnosed with the cellular variant of CMN

areas of hemorrhage and necrosis. Histologically, these tumors demonstrated nuclear atypia, high mitotic rate and increased nuclear/cytoplasmic ratio. Biologically this subgroup was more likely to invade local structures and recur following resection. Recently, molecular analysis has identified a t(12;15)(p13;q25) translocation in the cellular variant that results in a ETV6-NTRK3 fusion gene product [9, 10]. This translocation is not seen in the classic variant, but an identical gene fusion product has been reported in infantile fibrosarcoma [10]. This latter tumor is morphologically similar to cellular CMN, affects the same age group and shares an association with trisomy 11 [10].

While some studies have shown a slight female predominance [3], others have suggested that the tumor occurs more frequently in males [11]. Our study showed an equal sex distribution and, on the basis of current evidence, it seems unlikely that there is a significant difference in the incidence of CMN between the sexes.

Prenatal detection of the tumor is often possible by US, as was the case in 12 of the children in our study. Detection of the tumor as early as at 26 weeks of gestation has been reported [12]. The mass is generally of heterogeneous echogenicity and often indistinguishable from the kidney [6]. Polyhydramnios and premature labor are frequent associations [6]. Postnatally, 90% of tumors are discovered in the first 3 months of life [13]. While classic CMN is usually detected in the neonatal period, cellular CMN generally presents at a later age [3] and is therefore often larger. This was confirmed in our study, with a significant difference in the age at presentation between the two groups.

Abdominal radiographs appear to be generally nonspecific, with abdominal distension appearing to be the major finding. Displacement of bowel to one side may help to localize the tumor but adds little else to the initial evaluation. Typically, calcification within the tumor has not been identified on plain radiographs [4]. Previous studies have highlighted the key role US plays in the initial investigation of CMN [3, 4]. Cystic spaces and complex areas of increased echogenicity are more common in the

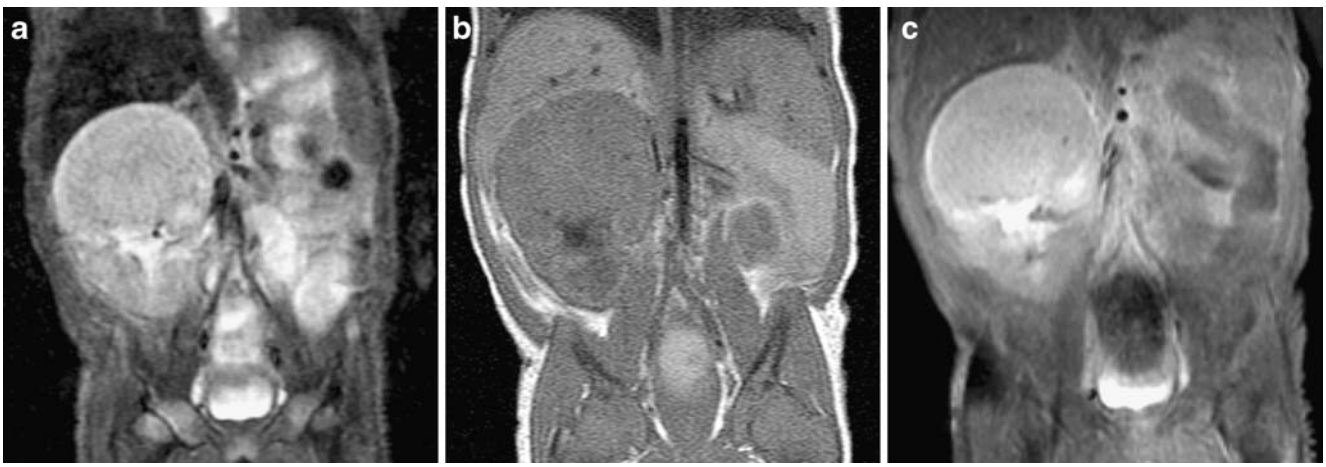

Fig. 7 A large mass arising from the upper pole of the right kidney in a 12-year-old boy. Pathology was consistent with classic CMN. **a** Coronal inversion recovery sequence demonstrates a homogeneous high-signal mass. **b** Coronal T1 sequence. A solid, homogeneous low-signal mass is seen. **c** Coronal T1 image after gadolinium administration. There is smooth, uniform enhancement of the tumor

cellular variant of CMN [3]. On examination of the gross specimens, these correspond to the areas of cystic/necrotic change and hemorrhage, respectively. In particular, US appears to be the most sensitive modality in identifying cystic components.

A concentric hyperechoic and hypoechoic ring pattern surrounding the tumor was originally described by Chan et al. in 1987 [3]. This pattern was seen in four out of the five infants in the study with classic CMN, but not in any of the children with the cellular variant. On microscopy, dilated blood vessels and entrapped nephrons were seen at the periphery of the tumor. A subsequent study highlighted blood flow within this ring on color and spectral Doppler [4], again only in patients with classic CMN. In our study, however, this sign was only seen in 7 of the 12 children with classic CMN, and was also seen in three children with a pathological diagnosis of cellular CMN. Therefore, it appears that while the ring is certainly more common in classic CMN, it is by no means universally identified or truly specific.

Prior studies examining the CT findings in CMN have also demonstrated varied appearance according to the pathological type. Classic CMN characteristically appears as a large, uniform, soft-tissue mass with minimal, predominantly peripheral enhancement [4, 14]. However, the enhancement pattern can often be focal and, particularly in cellular CMN, necrosis and hemorrhage can make the differentiation from Wilms tumor quite difficult [14]. The enhancement in the mass may be related to trapped functioning nephrons [7]. In our study, CT appeared to be less sensitive in detecting cystic areas than US, but focal areas of hemorrhage were more readily appreciated.

The MRI appearances of CMN appear to be quite variable according to the isolated reports in the literature. The tumor has been described as of low signal intensity on T1 imaging before and after gadolinium administration [15] to mixed signal intensity on T1 [16]. Similarly on fluid-sensitive sequences, the mass has been described as of markedly low signal in comparison to surrounding renal parenchyma [5] to predominantly high signal [16]. In our series, all of the tumors were of low signal intensity on T1, with focal areas of T1 shortening due to hemorrhage. The solid components of the masses were invariably bright on fluid-sensitive sequences, but demonstrated variability in enhancement on administration of contrast agent.

The differential diagnosis of CMN would include other renal and nonrenal tumors. Wilms tumor remains the most common renal tumor of childhood, but fewer than 2% present at less than 3 months of age [17]. Association with congenital syndromes or anomalies and the presence of bilateral tumors increase the likelihood of Wilms tumor [17]. On imaging, the tumor is often indistinguishable from CMN, particularly the cellular variant, although evidence of vascular invasion and pulmonary metastases (seen in up to 85%) are much more suggestive of Wilms tumor [13]. Other malignant renal tumors such as clear-cell sarcoma and rhabdoid tumors are much rarer, especially in infancy [17].

Nephroblastomatosis is usually readily distinguishable from CMN by the presence of multifocal and often bilateral solid masses. Accompanying findings include the presence of a Wilms tumor and association with Beckwith-Wiedemann, Denys-Drash or WAGR syndromes [13, 14]. Multilocular cystic renal tumor can be difficult to differentiate from a predominantly cystic CMN. Seen predominantly in boys, it occurs in the age range of 3 months to 4 years, overlapping with that of cellular CMN [13]. Imaging demonstrates a multiloculated, cystic mass with enhancing septations [14]. Ossifying renal tumor of infancy is a rare, usually small mass, arising from the renal medulla consisting of an osteoid core, osteoblasts and spindle cells [14, 17]. Usually at least partially ossified, these infants often present with hematuria [14].

The main nonrenal tumor in the differential diagnosis is neuroblastoma, commonly arising from the adjacent adrenal gland. However, the extrarenal origin of the mass can usually be confirmed by imaging, with associated displacement of the adjacent kidney. Additional differentiating features include encasement by neuroblastoma of the adjacent blood vessels and calcification, seen in more than half of neuroblastomas, but not a feature of CMN.

The review of the imaging findings allows us to recommend a plan of imaging investigation. The most appropriate initial study is an US examination, which helps to localize and define the nature of the mass. In the majority of patients, cross-sectional imaging will also be required to assess the site of origin of the lesion, local extension and impact on surrounding structures. The investigation of choice would be an MRI scan due to its multiplanar capabilities, high sensitivity for both hemorrhage and cystic changes and lack of radiation. In patients in whom neuroblastoma is also within the differential, this can also assess the extension of tumor into the neural foramen or spinal canal. The main disadvantage of MRI examination in this age group is often the requirement for sedation or general anesthesia. In terms of imaging alone, a CT study, particularly with multislice volumetric acquisition, can provide an alternative to the MRI examination. The rapid nature of the study often obviates the need for sedation. However, one has to account for the significant impact of radiation exposure at this early age and optimize imaging parameters if a CT scan is necessary [18]. In addition, precontrast scanning is rarely required in the investigation of CMN.

In conclusion, CMN varies markedly in appearance, ranging from completely solid to largely cystic. To a large

extent the appearance seems to be determined by the pathological type of the tumor. Although there are no absolutely specific imaging features, findings suggestive of the classic variety include a vascular ring and a large, solid component in the tumor. In comparison, tumors with multiple cystic areas and foci of hemorrhage are much more likely to be consistent with cellular CMN on histology. The imaging appearance seems to be largely consistent across the various imaging modalities and correlates well with the pathological findings.

References

1. Bolande RP, Brough AJ, Izant RJ Jr (1967) Congenital mesoblastic nephroma of infancy. A report of eight cases and the relationship to Wilms' tumor. Pediatrics 40:272–278
2. Joshi VV, Kay S, Milsten R et al (1973) Congenital mesoblastic nephroma of infancy: report of a case with unusual clinical behavior. Am J Clin Pathol 60:811–816
3. Chan HS, Cheng MY, Mancer K et al (1987) Congenital mesoblastic nephroma: a clinicoradiologic study of 17 cases representing the pathologic spectrum of the disease. J Pediatr 111:64–70
4. Kelner M, Droulle P, Didier F et al (2003) The vascular "ring" sign in mesoblastic nephroma: report of two cases. Pediatr Radiol 33:123–128
5. Puvaneswary M, Roy GT (1999) Congenital mesoblastic nephroma: other magnetic resonance imaging findings. Australas Radiol 43:532–534
6. Irsutti M, Puget C, Baunin C et al (2000) Mesoblastic nephroma: prenatal ultrasonographic and MRI features. Pediatr Radiol 30:147–150
7. Kirks DR, Kaufman RA (1989) Function within mesoblastic nephroma: imaging–pathologic correlation. Pediatr Radiol 19:136–139
8. Beckwith JB (1970) Mesenchymal renal neoplasms of infancy. J Pediatr Surg 5:405–406
9. Anderson J, Gibson S, Sebire NJ (2006) Expression of ETV6-NTRK in classical, cellular and mixed subtypes of congenital mesoblastic nephroma. Histopathology 48:748–753
10. Henno S, Loeuillet L, Henry C et al (2003) Cellular mesoblastic nephroma: morphologic, cytogenetic and molecular links with congenital fibrosarcoma. Pathol Res Pract 199:35–40
11. Geller E, Smergel EM, Lowry PA (1997) Renal neoplasms of childhood. Radiol Clin North Am 35:1391–1413
12. Apuzzio JJ, Unwin W, Adhate A et al (1986) Prenatal diagnosis of fetal renal mesoblastic nephroma. Am J Obstet Gynecol 154:636–637
13. Lowe LH, Isuani BH, Heller RM et al (2000) Pediatric renal masses: Wilms tumor and beyond. Radiographics 20:1585–1603
14. Riccabona M (2003) Imaging of renal tumours in infancy and childhood. Eur Radiol 13(Suppl 4):L116–L129
15. Rieumont MJ, Whitman GJ (1994) Mesoblastic nephroma. AJR 162:76
16. Wootton SL, Rowen SJ, Griscom NT (1991) Pediatric case of the day. Congenital mesoblastic nephroma. Radiographics 11:719–721
17. Glick RD, Hicks MJ, Nuchtern JG et al (2004) Renal tumors in infants less than 6 months of age. J Pediatr Surg 39:522–525
18. Olsen ØE, Gunny R (2006) Is there a role for CT in the neonate? Eur J Radiol 60:233–242